A comparison of UV intensities calculated by spherical-atmosphere radiation transfer codes: Application to the aerosol corrections

I. Petropavlovskikh,[1] R. Loughman,[2] J. DeLuisi,[3] and B. Herman[4]

Abstract. Various spherical radiative transfer (SRT) computer codes that model ultraviolet (UV) sky intensities incident at the Earth's surface are compared for clear-sky (Rayleigh scattering and ozone absorption) and hazy-sky (stratospheric volcanic aerosol, Rayleigh scattering, and ozone absorption) atmospheric conditions. Calculated sky intensities using Dave vector (pseudospherical), Dave scalar (pseudospherical), Herman's vector (full spherical), and Herman's scalar (full spherical) codes are compared for various parameters including solar zenith angle, direction of view, and wavelength. The differences in the calculated downward UV intensities are believed to arise from the differences in the code geometries and the neglect of polarization effects. The difference between downward UV intensities is within $\pm 15\%$ for clear-sky conditions and between -30 and 18% for hazy-sky conditions. The results of comparisons suggest that an experiment should be conducted to measure UV sky intensities for clear-sky conditions, with minimal aerosol, to test the quality of the radiative transfer codes with actual observations. The Dave scalar radiative transfer code has been used in the past to calculate aerosol error corrections to Umkehr measurements. To evaluate the accuracy of these calculations, we performed a set of comparisons with results of various spherical radiative transfer codes. Ground level sky intensities were calculated for various solar zenith angle directions, for a vertically inhomogeneous Rayleigh atmosphere with ozone absorption, including and excluding stratospheric aerosols. For 0.11 stratospheric aerosol optical thickness, the method for calculating stratospheric aerosol errors to retrieved Umkehr ozone profile predicts either -22% or -32% error in layer 8 depending on whether vector or a scalar radiative transfer code had been used. The calculations were also used to study the effect of full spherical and pseudospherical forward model differences on Umkehr ozone profile retrievals. The difference in retrieved ozone profiles was found to be within $\pm 4\%$ for clear-sky conditions and up to 13% in layer 8 for hazy-sky conditions. The results of these comparisons suggest that further improvements to the profile retrieval and stratospheric aerosol error calculations could be made using a fully spherical RT code that accounts for polarization.

1. Introduction

Dave's [1972a] scalar (DS) radiative transfer code has been used in the past to calculate aerosol error corrections to Umkehr measurements [*Dave et al.*, 1979; *DeLuisi et al.*, 1989; *Mateer and DeLuisi*, 1992]. Up to now, an examination of uncertainties in the Dave-Mateer (DV) pseudospherical vector code [*Dave*, 1964, 1972b] used for the Umkehr ozone profile retrieval algorithm and the aerosol error calculations arising from the use of Dave's pseudospherical atmosphere scalar code has not been done. To evaluate the accuracy of these codes, we performed a set of comparisons with a number of codes, namely *Herman et al.* [1995] full-spherical vector (HV)

code, *Herman et al.* [1994] full-spherical scalar (HS) code, Dave's pseudo-spherical atmosphere scalar (DS) [1972a], and vector (DV) codes [1972b].

The term "pseudospherical" means that attenuation of the incident solar light is computed using primary scattering spherical geometry, and the higher-order scattering calculations are done with a vertical system of plane-parallel homogeneous layers [*DeLuisi and Mateer*, 1971]. The term "fully spherical" means that all radiative transfer (RT) calculations are done using spherical geometry to represent more appropriate physics in the modeled atmosphere. The "fully spherical" code calculates the attenuation of the solar beam to the proper point for every line of sight, while the "pseudospherical" code calculates the attenuation of the solar beam once to every altitude on a single zenith and uses these values at each line of sight. This distinction is the most important cause of the differences in the results of the codes (see further discussion).

The term "vector code" (which computes all four Stokes parameters) means that polarization is fully taken into account. Conversely, the term "scalar code" means that polarization is not included. Because the *Herman et al.* [1995] fully spherical vector code is the most advanced of the other codes

---

[1]CIRES, University of Colorado, Boulder.
[2]Cooperative Center for Atmospheric Science and Technology, University of Arizona, Tucson.
[3]National Oceanic and Atmospheric Administration ARL/SRRB, Boulder, Colorado.
[4]Institute of Atmospheric Physics, University of Arizona, Tucson.

used in this investigation, it is believed to be an appropriate reference for comparison.

Polarization affects ultraviolet (UV) transmission by producing distinguishable (measurable) modification to the scattered radiation. The observed effect displays wavelength, azimuth, and solar zenith angle (SZA) dependencies. For example, in a Rayleigh atmosphere the minimum degree of polarization is in the vicinity of the Sun's direction. The maximum is located in the antisolar plane at ~90° from the Sun's direction [Coulson, 1988]. When the Sun is near the horizon, the maximum degree of polarization is observed near the zenith. As the Sun moves across the sky, the maximum degree of polarization moves from the zenith toward the antisolar horizon. Chadrasekhar [1960] illustrated the effect of replacing the exact Stokes treatment of polarization with the Rayleigh phase function only. For diffuse reflection from a semi-infinite atmosphere he illustrated the dependence of the total reflected intensities as a function of an angle of view and SZA. His results demonstrate that for a small SZA the calculated intensity in the nadir or zenith direction using the scalar Rayleigh phase function underestimates the intensity obtained when using the exact treatment of scattering by linear transfer of the Stokes parameters. The results are reversed when the Sun moves toward the horizon and passes ~50° SZA. Herman et al. [1995] obtained similar results in a study of the reflected intensities at the top of the atmosphere in the solar plane as a function of viewing angle and SZA. Mishchenko et al. [1994] discussed errors caused by neglect of polarization in intensities for Rayleigh atmospheres of different optical thickness and single-scattering albedo. They compared intensities derived from scalar and vector radiative transfer equations as functions of SZA and angle of scattering. The largest differences found between scalar and vector intensities were caused by "the scattering paths involving right scattering angles and right-angle rotations of the scattering plane" [Mishchenko et al., 1994].

2. Description of Intercomparisons

The following information summarizes the selective specifications for intercomparisons. The standardized atmosphere is composed of altitude profiles of pressure, midlatitude, springtime ozone, and elevated stratospheric aerosol. Total ozone is fixed at 350 Dobson units (DU) (0.350 atm cm), and ground level pressure is 1013.250 mbar. Zero surface albedo is used for RT calculations. Calculations of direct solar flux and sky intensities incident at the Earth surface are performed for ozone absorbing and Rayleigh/aerosol scattering in a spherical atmosphere at solar zenith angles 60°, 65°, 70°, 74°, 75°, 77°, 80°, 83°, 84°, 85°, 86.5°, 88°, 89°, and 90°. Since the application of the identical atmospheric structure is crucial for valid comparisons [Caudill et al., 1997], great care was taken to eliminate atmospheric layer system differences among the RT codes.

The normalized transmitted monochromatic direct-beam flux incident on a flat surface is defined as

$$F_{\text{dir}}(\mu_0) = \mu_0 \pi \exp(-\tau),$$

where μ_0 is the cosine of the solar zenith angle θ_0 (angle between direction to the Sun and the zenith vector of the observer's position at the surface), τ is the slant total optical depth of the spherical atmosphere in the direction of the Sun, and the extraterrestrial solar flux is normalized to $\pi = 3.141591$ which eliminates the need to carry it through the calculations. Spherical Earth radius is 6371 km.

Table 1. Spectral Absorption and Scattering Parameters

Wavelength, nm	Rayleigh-Scattering Coefficient β, (atm)$^{-1}$	Ozone-Absorbing Coefficient α, (atm cm)$^{-1}$
311.5	1.0362	2.1960
332.4	0.7845	0.1151

Zenith-sky intensity is defined as the intensity of the radiation due to all orders of scattering in the direction of the observation, $\theta = 0°$. Intensity is defined in units of energy per unit area per unit time per unit wavelength per unit solid angle (steradian).

Calculations were performed for two wavelengths 311.5 and 332.4 nm, also known as the Dobson C-pair. Spectral atmospheric parameters such as ozone-absorption and Rayleigh-scattering coefficients are listed in Table 1 [Mateer and De-Luisi, 1992].

Two stratospheric aerosol extinction profiles were taken from SAGE II data, first year (elevated aerosol) and second year (diminished aerosol) after the Pinatubo eruption (June 1991). Stratospheric aerosol optical thickness was estimated as high as 0.1 at 525-nm wavelength (maximum at 19.5 km) when the Pinatubo eruption cloud passed over the middle latitudes in January 1992, and 0.01 (maximum at 17.5 km) (also reported by DeLuisi et al. [1989] for the El Chichón aerosol), about twice background observed two years later. The profiles are zonally averaged between 40° and 50° N latitude. Aerosol optical properties for the Mie-scattering calculation were defined as a normalized lognormal size distribution given by

$$\frac{dn(r)}{dr} = \frac{1}{\sqrt{2\pi}r \ln\sigma} \exp\left[-\frac{\ln^2\left(\frac{r}{r_m}\right)}{2 \ln^2\sigma} \right],$$

where r_m is the mode radius; σ is the geometric standard deviation of width of the distribution. Values of size distribution parameters typical for stratospheric aerosols, such as $r_m = 315$ nm, $\sigma = 1.36$, and a refractive index of $1.47 - 0.00i$ representing particles of 75% water solution of H_2SO_4 [D'Almeida, 1991], were used in the computation.

3. Rayleigh Atmosphere

3.1. Polarization Effect in UV RT Modeling

To illustrate the effect of UV polarization at the ground, we compared intensity calculations performed with and without polarization using HV and HS codes. Figure 1 shows the hemispheric distribution of the percent error in polar and azimuth angle directions, referenced to the HV code, for 311 and 332 nm, and for SZA of 80°. These errors are associated with neglecting the polarization effect in the radiative transfer model. The pattern of errors depends on SZA. Figure 2 illustrates the SZA dependence of the error at a fixed 55° polar angle, calculated for 311 nm and for 350 DU total ozone. In general, the magnitude of the error is largest in the solar plane, although at large SZAs, the error reaches its maximum at 90° azimuth angle.

The magnitude of the error does not change significantly with wavelength except at large SZA. Whereas attenuation of UV is stronger at the shorter wavelength due to ozone absorption (mostly in the middle stratosphere), most of the multiple

scattering occurs in the dense lower atmosphere. Furthermore, molecular scattering and ozone absorption decline with increasing wavelength in the UV part of the solar spectrum. Thus their combined contribution to the sky intensity calculated at the two wavelengths is nearly comparable except at large SZA where the scattering contribution outweighs absorption.

3.2. Pseudospherical Versus Fully Spherical

The difference in the intensity calculated by DV and HV codes for outgoing radiation at the top of the atmosphere has been examined by *Caudill et al.* [1997]. They found three major factors responsible for the differences in the results of these two codes: (a) the attenuation of the incident solar radiation, (b) the attenuation of the scattered light, and (c) integrated optical path. The same three factors would affect the difference in modeled radiation estimated at the ground level. Figure 3 presents results of this study which are somewhat consistent with results of *Caudill et al.* [1997, Figure 6a]. We found that for a low-Sun condition, and at 311-nm wavelength, the DV code underestimates intensity in the solar side quadrant (as much as −4.4% in forward scattering direction for 80° SZA) and overestimates the antisolar side intensity (maximum 4%) relative to the HV code. The difference between codes at 311 nm increases with SZA, up to −14% in the solar quadrant, and 10% in the antisolar quadrant at 90° SZA. However, when the Sun is high, the DV code behaves very well and only slightly overestimates radiation at any angle of view. For example, for a Sun at 60° SZA the differences are found to be as small as −0.5% in the vicinity of the zenith direction while increasing to 1% in antisolar quadrant. The difference in intensities calcu-
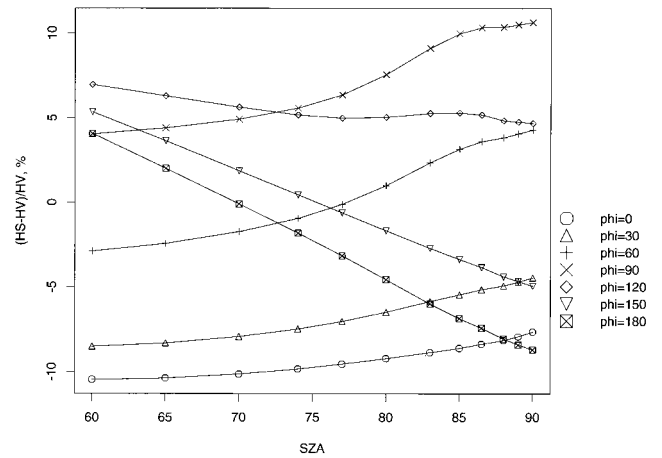

Figure 2. Percent difference between the HS and HV (HV is the reference) model calculations of sky intensity at the ground as a function of solar zenith angle for 311-nm wavelength, 350 DU total ozone, and 55° polar angle. Phi is the azimuth angle.

lated by DV code relative to HV code is smaller at 332-nm than at 311-nm wavelength except at large SZAs. Figure 3b shows the differences at 332 nm and 80° SZA ranging from −1 to 3%. The difference between the codes at 332 nm increases with SZA from less than a percent at 60° SZA to a maximum of ±15% at 90° SZA, while the DV code overestimates the HV code over most of the hemispheric area of view.

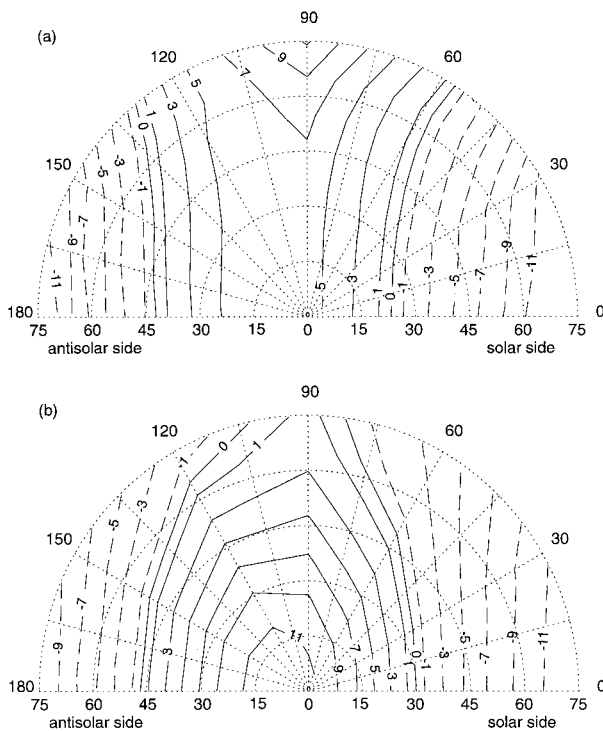The difference between radiance calculated by the pseudo-

Figure 1. Percent difference in the diffuse intensity versus viewing direction in polar angle (abscissa) and azimuth angle (circumference) at the ground between the HS and the HV models (HV is the reference) for 80° SZA, 350 DU total ozone, Rayleigh atmosphere: (a) 311-nm and (b) 332-nm wavelengths.
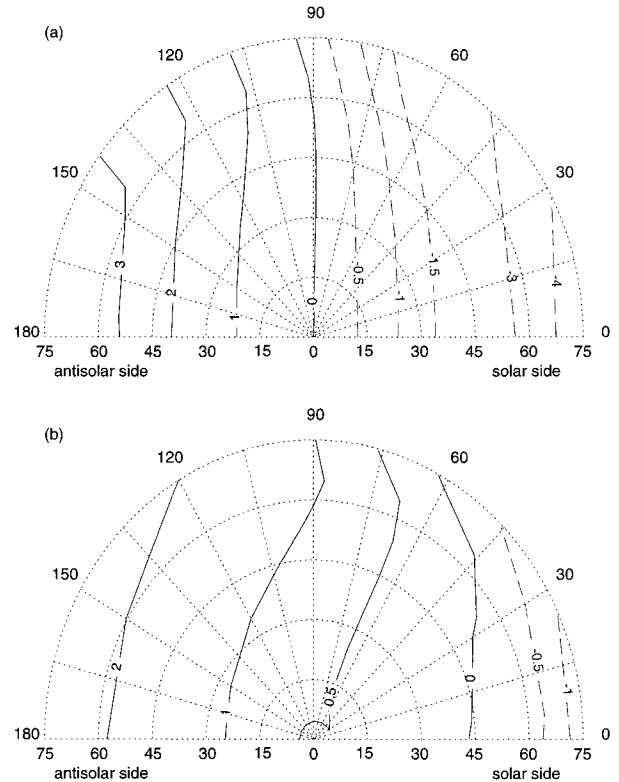

Figure 3. Percent difference between the DV and the HV models (HV is the reference) in the diffuse intensity at the ground for 80° SZA, 350 DU total ozone, (a) 311-nm and (b) 332-nm wavelengths.
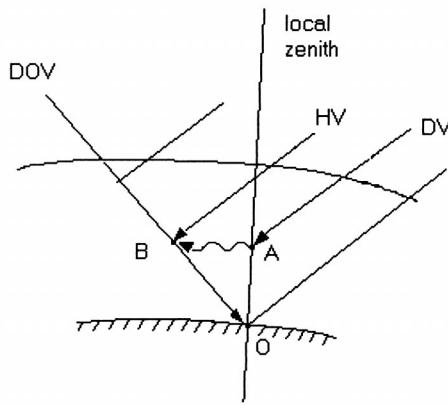
Figure 4. Difference in geometry of scattered light used in fully spherical (Herman vector) and pseudospherical (Dave vector) codes. DOV points direction of view, HV, and DV identify difference in geometry of incoming direct solar light used in Herman vector and Dave vector models, respectively.

spherical model (DV) and the spherical model (HV) for satellite observation geometry is described by *Caudill et al.* [1997]. The main reason for such a difference is found to be in the attenuation of the direct solar light or source function. For the single-scattering case, the overestimation/underestimation of the radiation is due to the difference in the optical path along which the direct solar radiation is attenuated in the DV or HV models before it is scattered. However, there is a distinct difference between satellite and ground-based observation geometry. Figure 4 shows ground-based observational point O that is located at the surface rather than at the top of the atmosphere as in the work of *Caudill et al.* [1997]. As shown in Figure 4, the line of a sight (line BO) intercepts the surface at the point of observation. In both codes the curvature of the atmosphere is properly accounted for in the single-scattering calculation. However, treatment of solar attenuation is done differently in the codes. Figure 4 displays the points at which the solar attenuation is calculated for one level along the line of sight BO using the HV code (point B) and the DV code (point A). In the DV code, attenuation of the solar light is calculated to the point A. Then, this incident intensity is used in the source function for a single-scattered radiation at point B. Thus the source function for solar radiation scattered along the line of sight BO is larger in the DV code than in the HV code. It is distinctly seen that on the antisolar side of the hemisphere the HV model has a longer optical path to the point of scattering (point B) than in the DV model (in which the optical path to the point A is instead used). Thus the DV code has more solar radiation to points along the line of sight than the HV code. This explains the overestimation of the ground intensity by the DV code in the antisolar section of the hemisphere. In the solar section the reasoning is similar with the opposite results.

The approximate calculation of the single scattering in the DV code causes an error of the opposite sign when the observer is at the top of the atmosphere. As noted above, the DV code calculates the solar beam attenuation to all levels along a single zenith, which is defined by the point at which the relevant line of sight intersects the surface of the Earth. The solar beam optical path lengths calculated to this single zenith are then applied to the points along the line of sight, which is not

strictly correct unless the zenith or the nadir is the chosen line of sight. The error associated with this approximation for the satellite case is clearly illustrated by *Caudill et al.* [1997, Figure 2a]. Solar beam attenuation is underestimated by the DV code in the solar section of the hemisphere and overestimated in the antisolar direction. As a result, the DV code overestimates the intensity in the solar section of the hemisphere and underestimates it in the antisolar section, as shown by *Caudill et al.* [1997, Figure 6].

The differences in the ground intensity originate from the differences in the geometry used in the pseudospherical and spherical models. Figure 5 shows the difference in calculated ground level sky intensities at 311 nm and 55° polar angle as a function of SZA and azimuth angle. The results seen in this figure are similar to the findings of *Caudill et al.* [1997] (see *Caudill et al.* [1997, Figure 8] for comparisons). Again, the effect at the ground is reversed in the solar and antisolar planes relative to the results at the top of the atmosphere (see discussion above). The magnitude of the error is less than 1% at SZA less than 70° and has a very small dependence in the azimuth direction. At SZAs larger than 70°, the difference between DV and HV codes increases almost exponentially with SZA and depends on azimuth direction. The magnitude of the difference is largest in the solar plane. At 332-nm, when the Sun is high, the difference becomes smaller which reflects a reduction of solar light attenuation prior to the scattering. When the Sun is near horizon, contribution of the multiple scattering to the intensity at the given angle of view is larger at 332 nm than at 311 nm. Therefore at 332 nm the difference in intensities caused by difference in geometry used in DV and HV codes increases at large SZAs.

3.3. Zenith-Sky Intensity

According to *Caudill et al.* [1997] the difference in the single-scattering calculation by the HV and DV codes vanishes for the nadir direction. Therefore this case eliminates one of the errors and allows for a study of other effects. Furthermore, zenith-sky intensity (ZSI) over the range of SZA of 60°–90° is the measurement used to retrieve ozone profile information in the Umkehr method.

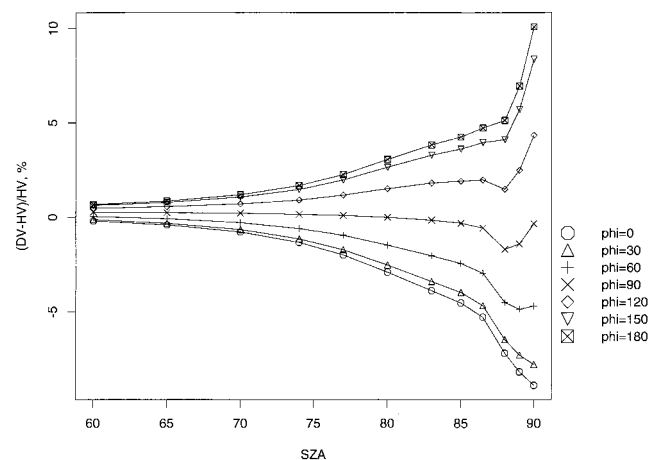For a Rayleigh atmosphere with ozone absorption, calcu-

Figure 5. Percent difference between the DV and HV models (HV is the reference) in the sky intensity at the ground as a function of solar zenith angle for 311-nm wavelength, 350 DU total ozone, and 55° polar angle.

lated ZSI using selected radiative transfer (RT) codes were compared with the DS code (the reference intensities). It was found that the differences among the results of all codes compared in this study depend on solar zenith angle (see Figure 6). Another characteristic feature of this plot is the similar behavior of all vector codes. For example, the vector codes (HV and DV) show very good agreement with each other with differences less than 1%. For high-Sun conditions (60° SZA) the DS code overestimates ZSI by less than 5% compared to the results of vector codes. For lower-Sun conditions (60° < SZA < 90°) it overestimates results of the vector codes by less than 11%. The failure to account for a polarization effect in the UV ZSI calculations produces errors that vary with SZA and wavelength and are in the range of 11%. Generally, for clear-sky conditions the DS UV ZSI is overestimated for low-Sun conditions.

The DS and HS codes are in agreement to better than 1% at all solar zenith angles. The small difference at large SZAs might be caused by different multiple-scattering geometry. Whereas the HS code applies spherical geometry for multiple-scattering calculations, the DS code uses the plane-parallel assumption for calculation of scattered radiation of the second and higher orders. The large difference (up to 11%) between HV (fully spherical) and HS (fully spherical) codes is attributed to polarization, which is included only in vector codes.

4. Hazy Atmosphere

4.1. Polarization Effect in UV

It has been commonly observed that following a strong volcanic stratospheric aerosol injection event, the sky in visible
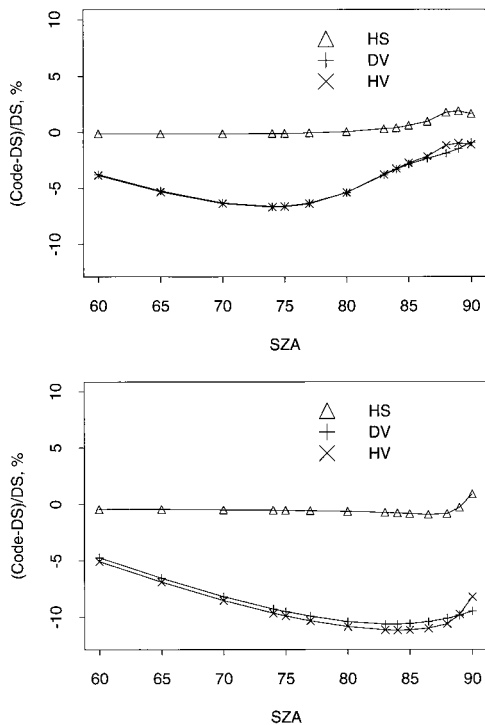

Figure 7. Same as Figure 1 but for stratospheric aerosol contamination.

Figure 6. Relative errors in zenith-sky intensity at the ground level calculated for (a) 311-nm and (b) 332-nm wavelengths using selected radiative transfer methods (shown in key) for a Rayleigh-scattering and ozone-absorbing (350 DU) atmosphere. Results of Dave scalar code are used as a reference.
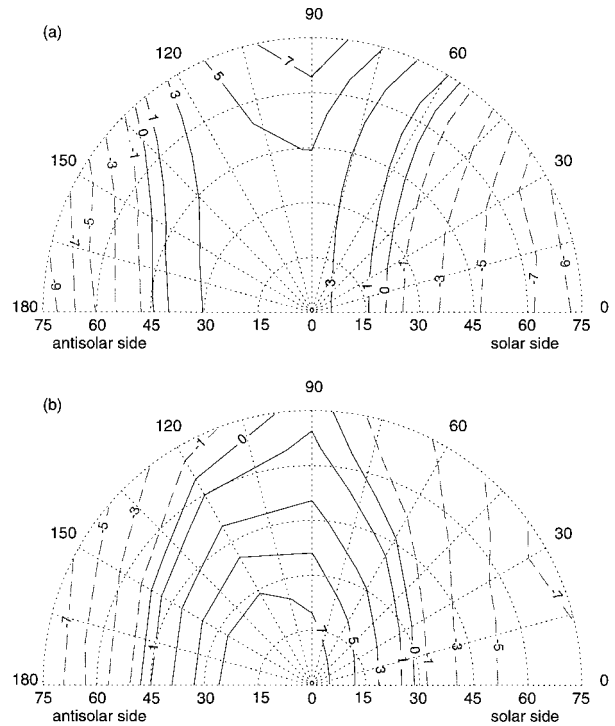
solar wavelength range appears "milky." At 311-nm wavelength, HV-modeled ZSI is increased relative to the nonaerosol atmosphere case with a maximum difference at about 80° SZA. The effect is similar to the Umkehr effect except that UV radiation is modified by the presence of the stratospheric aerosol layer, which is usually in close colocation with the ozone layer. In other words, UV radiation is scattered downward above the observer; the enhanced aerosol forward scattering increases the ZSI relative to the Rayleigh-scattering case. At 332-nm the HV modeled ZSI is increased when the Sun is high and is reduced when the Sun is low relative to the clear-sky case. The difference is caused by the difference in the ozone absorption at two wavelengths, with absorption at 311 nm being stronger than at 332 nm. As a result, the direct beam must propagate deeper into the atmosphere at 332 nm before stronger downward scattering occurs. When the Sun approaches horizon, the long slant path causes the direct beam to be further attenuated during volcanic events. The source function for the downward scattered intensity becomes weaker than for the nonaerosol case and, consequently, cannot contribute as much to the downward scattering. Therefore ZSI is decreased relative to the Rayleigh case.

When the Sun is high, the angular distribution of the differences in calculated sky intensity using the DV and HV codes (see Figure 7) is similar to the clear-sky case shown in Figure 1. The magnitudes of the differences become larger at large solar zenith angles when the contribution to scattered light from Rayleigh and aerosol particles becomes comparable with the ozone absorption. There is also a slight polarization effect in the direction toward the Sun in the solar plane. The differences in the direction of the Sun are relatively smaller in comparison with errors at adjacent angles of view. Figure 8 displays the percent difference between calculated ZSIs using HS and HV codes due to the neglect of the polarization effect
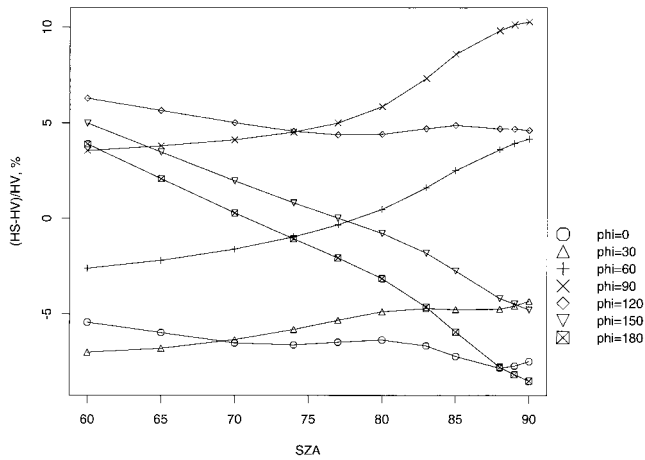
Figure 8. Same as Figure 2 but for stratospheric aerosol contamination.

as a function of SZA and azimuth angle, with polar angle fixed at 55°. The angular dependence of errors due to aerosols is similar to the clear-sky case shown in Figure 2, although the difference magnitudes are reduced, especially in the solar plane. Stratospheric aerosols enhance forward scattering in the UV and reduce the polarization effect in the direction of the peak-scattering contribution. This direction is coincident with direction toward the Sun when the Sun is high, and it is above the solar height when the Sun is low.
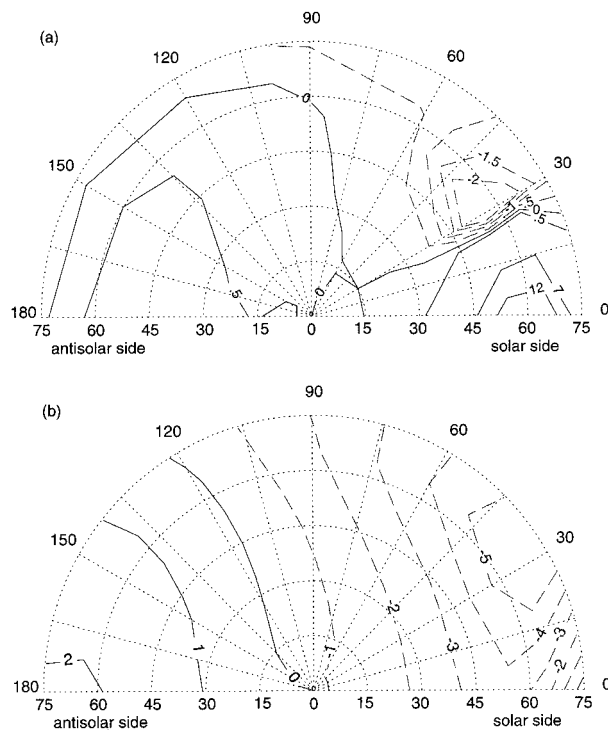

Figure 9. Percent difference between the DV and the HV models (HV is the reference) in the diffuse intensity for stratospheric aerosol contamination at the ground for 311 nm, 350 DU total ozone, (a) 60° SZA, and (b) 80° SZA.

4.2. Pseudospherical Versus Fully Spherical Vector Codes

For twilight conditions with stratospheric aerosols present, the difference in modeled sky intensities caused by the difference in geometry of the vector code multiple-scattering treatment can be significant (see Figure 9). This difference results from two effects and is a function of SZA. The effects are increased attenuation of the scattered light and truncation of the aerosol scattering contribution. It is also worth to note that no significant differences between DV and HV results at 60° SZA occur outside the forward peak region in Figure 9a. Also, Figure 9b has a pattern very similar to Figure 3a (same case but no aerosols) outside the forward peak region.

The difference between intensities calculated with the HV and the DV codes is enhanced in the direction from the Sun with some opposite effects at other azimuth angles outside the solar plane but at the same polar angle (see Figure 9a). The effect can be described as two peaks (one positive and one negative next to it) in the solar section of the hemisphere. The effect is greater at high Sun. When the Sun is near the horizon (see Figure 9b), the distinct peak disappears, while the difference in sky intensity is still larger in the direction toward the Sun. The primary reason for disagreement in the forward scatter direction is the large forward peak in the aerosol-scattering phase function at ultraviolet wavelengths. This feature causes the "solar aureole" (a region of enhanced brightness surrounding the solar disk) to form. The rapid variation in the phase function causes the radiance field to vary rapidly with direction, and specialized methods have been devised to allow accurate radiative transfer calculations in the solar aureole [cf. *Herman and Browning*, 1975; *Karp*, 1981; *Stamnes*, 1982; *Karp and Petrack*, 1983; *Nakajima et al.*, 1983; *Arao and Tanaka*, 1986; *Tonna et al.*, 1995]. Neither the DV nor the HV codes is optimized for the solar aureole problem in its standard mode of operation, and therefore neither code captures the radiance field in the solar aureole properly. Differences in the angular resolution of the DV and HV codes also may cause their output to disagree in the forward scattering direction but have almost no effect for other lines of sight.

Figure 10 illustrates the SZA effect at 55° polar angle. Results show strong overestimation of the DV code relative to the HV results (15%) in the solar plane at a SZA is close to the polar angle. There is also a characteristic negative difference at the 30° azimuth angle (−3%). This feature is present in the
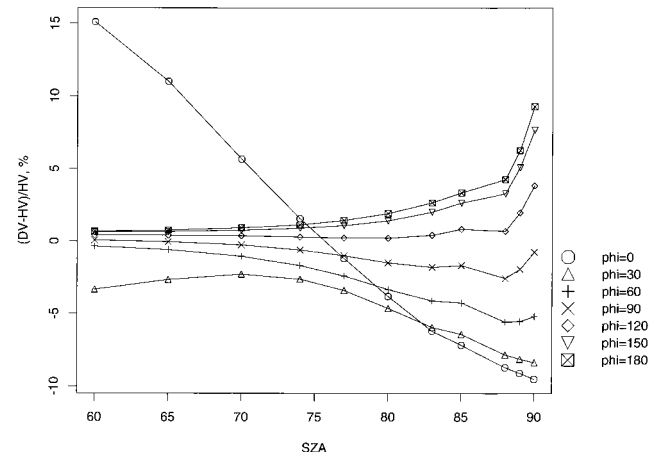

Figure 10. Same as Figure 5 but for stratospheric aerosol contamination.

differences calculated at both wavelengths. We believe that almost all of the forward peak differences could be attributed to the angular resolution differences between the codes.

4.3. Zenith-Sky Intensity

For hazy atmospheric conditions the difference in calculated ZSI using HV and DV codes relative to the results of DS code becomes less than that for Rayleigh atmosphere conditions. A low aerosol amount (results are not shown, optical thickness 0.01) produces only a small effect on the observed differences for all RT code results. However, enhanced aerosol amount (0.1) noticeably reduces discrepancies with the largest effect for the larger SZA (see Figure 11).

Vector codes (DV and HV) show very good agreement. Nonetheless, at 311-nm wavelength there is a 2% difference between ZSIs calculated at SZA 88° using DV and HV codes (see Figure 11a). Yet, at 332-nm wavelengths, solar zenith angle 88°, the DV code underestimates the HV code by about 4% (see Figure 11b). This discrepancy is caused by the difference between fully spherical (HV) and pseudospherical (DV) atmosphere treatment of the radiative transfer [*Caudill et al.*, 1997] which is enhanced at large SZA. It also has wavelength dependence due to increased contribution of the scattered light at the longer wavelength. Otherwise, the difference between vector codes is less than 1%.

At 311 nm the difference between ZSI calculated by HS and DS codes is less than 2% for enhanced aerosol at solar zenith angles larger than 85°. However, at 332 nm the DS code underestimates the results of the HS code as much as 8% at large SZAs. The cause of the difference between ZSI calculated by HS and DS codes at large SZAs (see discussion above) is most likely due to differences in the angular treatment of the scat-
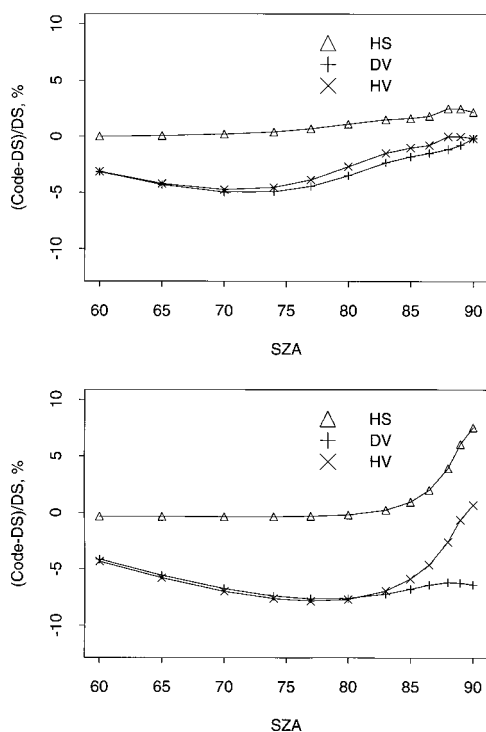

Figure 12. *N*-value difference between hazy and clear-sky atmospheric conditions calculated with four RT codes (shown in key) at selected solar zenith angles. Stratospheric aerosol optical depth is 0.11; aerosol profile was obtained from SAGE II observations.

tered light in the codes. Moreover, the contribution of the multiple-scattered light in ZSI increases with wavelength, increasing the difference between ZSIs calculated by HS and DS codes.

5. Umkehr Aerosol Error Calculation Sensitivity

Results from these comparisons permit an evaluation of the DS code accuracy for calculating the stratospheric aerosol error to Umkehr profile retrievals. From this investigation it is clear that there are some nonnegligible discrepancies between the results of a vector code and the scalar code used by *DeLuisi et al.* [1989]. Therefore the differences that have been uncovered in the present work could affect their Umkehr aerosol error correction calculation schemes.

Since the aerosol error calculations are based on a forward calculation method the results of the comparison to be made next will depend on the accuracy of the calculation method and not on an information-limited process such as finding an inverse. The next part of this investigation is concerned with a comparison of aerosol errors to the Umkehr ozone profiles calculated with the vector and scalar codes. The aerosol optical information remains fixed with altitude and wavelength.

The aerosol error is determined from RT calculations of the difference in *N* values ($N_{\text{aerosol}} - N_{\text{clear}}$, where $N = 100 \log I/I'$ and I' is ZSI at the shorter wavelength), each calculated at 14 Umkehr standard solar zenith angles (Figure 12). For details, see *DeLuisi et al.* [1989]. The Umkehr measurement is given in terms of the logarithm of the ratio of two zenith-sky intensities measured at the wavelengths 311 and 332 nm (the standard C-pair) as the solar zenith angle changes from 60° to 90°. It is well known that the maximum error sensitivity of Umkehr retrievals to atmospheric aerosol is in the upper Umkehr layers [cf. *Mateer and DeLuisi*, 1992; *Newchurch et al.*, 1994; *DeLuisi et al.*, 1996]. The largest Umkehr observation error due to aerosols is found at large solar zenith angles that also contribute to most of the ozone profile information in the upper layers. Furthermore, at solar zenith angles larger than 85° we find that the HV code yields significantly different results (up to 4 *N*-values) compared to the DS code. Therefore we could expect a large difference in calculated aerosol errors associated with the use of HV and the DS codes.

The results shown in Figure 12 are used to calculate the stratospheric aerosol error to retrieved Umkehr ozone profiles

Figure 11. As in Figure 6 but for hazy atmospheric conditions. The vertical profile of the elevated stratospheric aerosol extinction is taken from SAGE II data. Aerosol optical thickness is about 0.11.
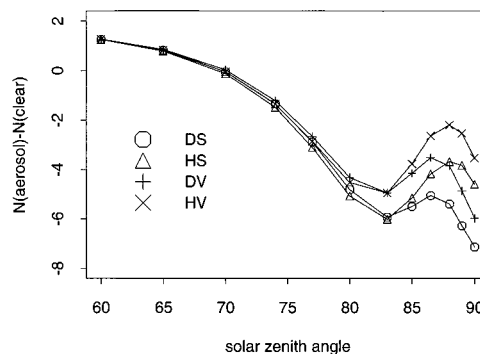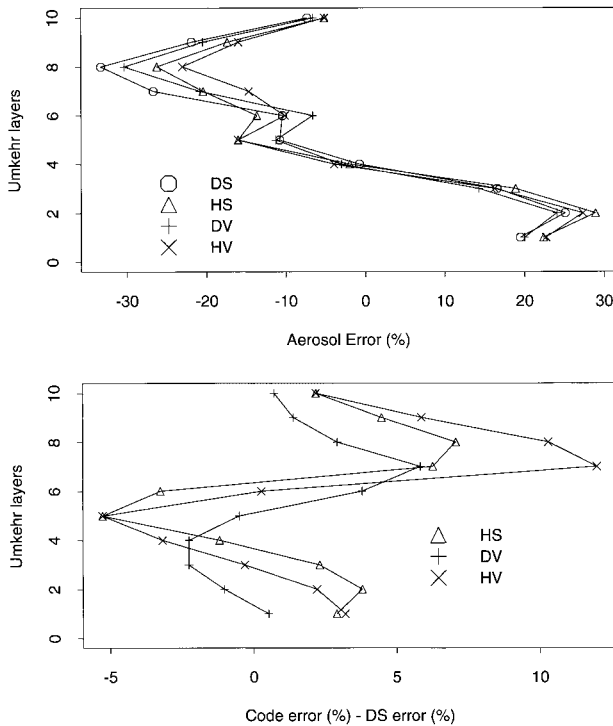
Figure 13. (a) Calculated stratospheric aerosol error to the new (1992) Umkehr algorithm retrieved ozone profile using results of Figure 12. (b) Residuals between ozone profile aerosol errors calculated using selected RT codes and the errors calculated with the DS code.
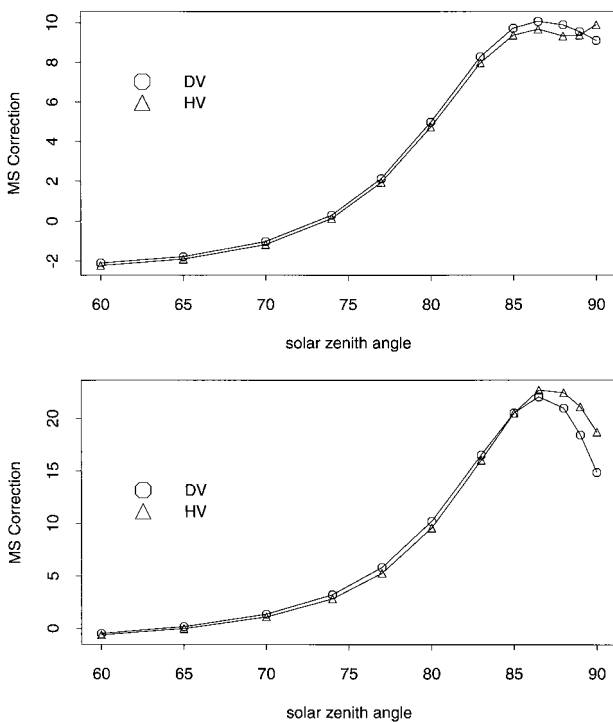

Figure 14. Multiple-scattering components in N values calculated using the DV and HV codes as a function of solar zenith angle: (a) for a Rayleigh atmosphere (clear) and (b) for Rayleigh atmosphere with stratospheric aerosols (aerosol).

by inverting each error function using the 1992 Umkehr ozone profile retrieval algorithm. To eliminate the effect of the first-guess ozone profile on the results of the Umkehr-retrieved ozone profile, the standard (midlatitude, spring, 350 DU total ozone) N values are perturbed by adding the difference in N values calculated with and without stratospheric aerosol. The aerosol optical thickness is 0.11 and represents the maximum El Chichón optical thickness observed in January 1983 over Boulder [*DeLuisi et al.*, 1989]. The standard and aerosol-perturbed N values are used to retrieve ozone profiles using the 1992 Umkehr algorithm. Aerosol errors to the retrieved ozone profile are calculated for each RT method (see Figure 13a). Overall, the difference among aerosol errors ranges between -5 and 12% when any other than the DS code is used to calculate N values (see Figure 13b). As expected, the calculated aerosol error using the DS code is overestimated in layer 7 by about 12% relative to results of the HV code. On the other hand, if one regards the HV results as the reference, then the absolute error of the DS code results becomes 85% too large. This finding was very gratifying because it appeared from simple empirical analysis (i.e., change in retrieved ozone profile with respect to change in observed aerosol optical depth) that the earlier DS code aerosol error computations were over-estimating the aerosol error.

Results from Figure 12 are also used to estimate the errors in the Umkehr ozone profile retrieval algorithm due to errors in the modeled multiple-scattering component of the zenith-sky intensity. The DV code models the multiple-scattering correction in the retrieved algorithm. The difference between N values, calculated using the DV and HV codes, is used to perturb the standard N-values (see above). The difference is then inverted to calculate ozone profile differences for clear sky as well as for hazy skies. Figure 14 illustrates the discrepancies in multiple-scattering components of the N values calculated using DV and HV codes for clear- and hazy-sky conditions. Multiple scattering here means secondary and higher orders of scattering. Figure 15 illustrates the effect of the difference in multiple-scattering treatments by DV and HV codes on Umkehr-retrieved ozone profile for clear and hazy atmospheric conditions. These ozone profile differences are related to larger DV code errors in layers 8 and 9 compared to the HV code (see Figure 13a). Differences range between -4
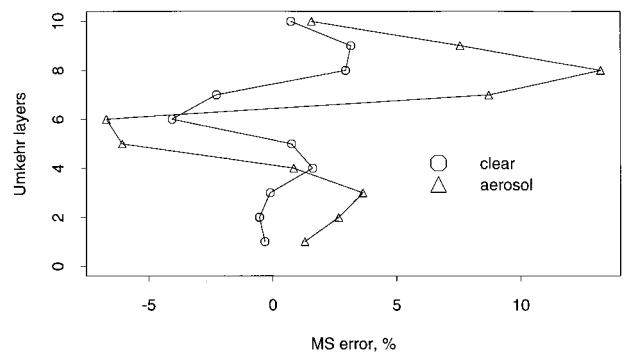

Figure 15. Percent change in the Umkehr-retrieved ozone profile caused by the difference in modeled multiple-scattering component of ZSI derived from results of the DV code in comparisons to the results of the HV code (DV is the reference) for clear sky and stratospheric aerosol (0.11 optical thickness) atmospheric conditions.

to 4% and −7 to 13% for clear sky and stratospheric aerosol conditions, respectively. The results of HV code are used as a reference. Again, multiple-scattering corrections to observed N-values used in the 1992 Umkehr retrieval algorithm [*Mateer and DeLuisi*, 1992] were originally calculated using the pseudo-spherical DV code. However, the results in Figure 15 for clear-sky conditions suggest possible small systematic errors in the Umkehr-retrieved ozone profile due to the errors in the multiple-scattering correction used in the Umkehr retrieval algorithm. These ozone profile errors are rather small and, for clear-sky conditions, are roughly of the order of magnitude of measurement errors. Nevertheless, for stratospheric aerosol conditions the multiple-scattering errors in retrieved ozone (see Figure 15) are of the same order of magnitude as the errors due to elevated stratospheric aerosol levels discussed above (see Figure 13). This could potentially affect the quality of the ozone profile retrievals and result in overestimation of aerosol corrections for Umkehr-retrieved ozone profiles. While we believe that the retrieval algorithm forward model differences seen here might not seriously impact ozone trends, the differences of the order of a few percent or more will be important when making comparisons with other types of ozone profile observational methods. For example, see the comparison by *Newchurch et al.* [1998] and by *Petropavlovskikh et al.* [1999], which shows that observed upper atmosphere Umkehr profiles display a similar pattern of systematically lower ozone concentration than those observed by the SBUV and the SAGE satellites. An in-depth study is needed to fully understand the implication of these preliminary results.

6. Conclusions

The results discussed in this paper uncover some significant problems with the pseudospherical atmosphere treatment of radiative transfer when UV sky intensities are modeled for low-Sun conditions. The comparisons show that the difference between off-zenith intensities calculated with pseudospherical and fully spherical vector codes varies with solar zenith angle, wavelength, and azimuth angle. For atmospheric conditions in the absence of aerosols these geometric errors are less than 1% for solar zenith angles less than 70°, while for large solar zenith angles, the errors can be as large as ±15%. However, differences in sky intensity calculations increase in the vicinity of the Sun when modeled for elevated volcanic stratospheric aerosol conditions. For such conditions (stratospheric aerosol optical thickness 0.11) the comparisons show that the difference in UV sky intensities calculated using DV (pseudospherical) and HV (fully spherical) codes is the largest in the solar plane, in the vicinity of the Sun (ranging between −32 and 18%). However, both codes are not optimized for the solar aureole problem in its standard mode of operation, and therefore neither code can capture the radiance field in the solar aureole properly. Differences in the angular resolution of the DV and HV codes cause their output to disagree in the forward scattering direction but have almost no effect for other lines of sight.

The modeling errors associated with the neglect of polarization are discussed in this paper. It is shown that these errors can be comparable to the errors encountered with the pseudospherical versus fully spherical atmosphere treatment, i.e., within 20%, and depend on solar zenith angle, polar angle, azimuth angle, and wavelength. The geometric modeling errors and polarization errors can be added to define the effect of both error types. The range of errors in zenith-sky intensities due to the polarization is within 1.5 N- within 1.5 N-values, while geometrical errors are found to be within 2.5 N-values. The range of both errors is within 4 N-values.

Selected radiative transfer (RT) codes are used in the investigation to validate the accuracy of the Dave scalar (DS) code. The series of zenith-sky intensities are calculated at the ground level, at various solar zenith angles, and for a Rayleigh-scattering and ozone-absorbing atmosphere, with and without stratospheric aerosols present. Results of comparisons show that there is an overall 1% difference between selected vector codes. The difference between zenith-sky intensities calculated using all RT codes and the DS code depends on solar zenith angle (SZA) and wavelength and varies within a 15% range. The results of comparisons suggest that an experiment should be conducted to measure UV sky intensities for clear-sky conditions, with minimal aerosol, to test the quality of the radiative transfer codes with actual observations.

For the calculation of the Umkehr stratospheric aerosol error (optical thickness 0.11), a maximum difference of nearly 4 N-values was accorded to the different RT codes. The modeled ozone profile errors of stratospheric aerosol effect are sensitive to the RT code used. It was determined that ozone profile errors calculated with HV code can differ almost twice in magnitude from errors calculated with the DS code.

The difference in the Umkehr-retrieved ozone profile due to the difference in the forward model used to calculate the multiple-scattering component of the zenith-sky intensity was estimated for a special case. It was determined that maximum ozone profile errors can be found in layers 6 and above ranging from ±4% for clear-sky atmospheric conditions and between −7 and 13% for elevated stratospheric aerosol conditions.

The update of the forward model of the Umkehr retrieval algorithm to incorporate improved modeling of zenith-sky intensities is an option that needs to be considered. This will enable the Umkehr algorithm to use a local geophysical temperature/pressure climatology for ozone profile retrievals at individual stations and help to reduce retrieval noise associated with the temperature profile variance. Therefore the quality of the individually retrieved ozone profiles could be potentially improved. Further study is needed to assess the internal consistency of the Umkehr-retrieved ozone profiles and to compare them with other remote sensing ozone measurements. Finally, it is our belief that the suggested changes in the ozone profile retrieval algorithm will have at most only slight impact on trend analysis performed on the retrieved ozone profiles. However, improved calculations of stratospheric aerosol errors might have a greater effect on trend analysis.

References

Arao, K., and M. Tanaka, Dependence of the solar aureole upon the optical properties of aerosols and albedo of the ground surface, *J. Meteorol. Soc. Jpn.*, *64*, 743–753, 1986.

Chandrasekhar, S., *Radiative Transfer*, pp. 42,262–42,265, Dover, Mineola, N. Y., 1960.

Caudill, T. R., D. E. Flittner, B. M. Herman, O. Torres, and R. D. McPeters, Evaluation of the pseudospherical approximation for backscattered ultraviolet radiances and ozone retrieval, *J. Geophys. Res.*, *102*, 3881–3890, 1997.

Coulson, K. L., *Polarization and Intensity of Light in the Atmosphere*, 596 pp., A. Deepak, Hampton, Va., 1988.

D'Almeida, G. A., P. Koepke, and E. P. Shettle, *Atmosphere Aerosols: Global Climatology and Radiative Characteristics*, A. Deepak, Hampton, Va., 1991.

Dave, J. V., Multiple scattering in a non-homogeneous atmosphere, *J. Atmos. Sci.*, *22*, 273, 1964.

Dave, J. V., Development of programs for computing characteristics of ultraviolet radiation, in *Scalar Case*, *Tech. Rep.*, IBM Corp., Fed. Syst. Div., Gaithersburg, Md., 1972a.

Dave, J. V., Development of programs for computing characteristics of ultraviolet radiation, in *Vector Case*, *Tech. Rep.*, IBM Corp., Fed. Syst. Div., Gaithersburg, Md., 1972b.

Dave, J. V., J. J. DeLuisi, and C. L. Mateer, Results of comprehensive theoretical examination of the optical effects of aerosols on the Umkehr measurement, *Spec. Environ. Rep. 14*, p. 15, World Meteorol. Organ., Geneva, 1979.

DeLuisi, J. J., and C. L. Mateer, On the application of the optimum statistical inversion technique to the evaluation of Umkehr observations, *J. Appl. Meterol.*, *10*, 328–334, 1971.

DeLuisi, J. J., D. U. Longenecker, C. L. Mateer, and D. J. Wuebbles, An analysis of northern middle-latitude Umkehr measurements corrected for stratospheric aerosols for 1979–1986, *J. Geophys. Res.*, *94*, 9837–9846, 1989.

DeLuisi, J. J., I. V. Petropavlovskikh, C. L. Mateer, An evaluation of the uncertainties in estimating stratospheric aerosol errors to retrieved Umkehr ozone profiles, in *Proceedings of the XVIII Quadrennial Ozone Symposium in L'Aquila, Italy*, edited by R. Bojkov and G. Visconti, 115 pp., 1996.

Herman, B. M., and S. R. Browning, The effect of aerosols on the Earth-Atmosphere albedo, *J. Atmos. Sci.*, *32*, 1430–1445, 1975.

Herman, B., A. Ben-David, and K. J. Thome, Numerical technique for solving the radiative transfer equation for a spherical shell atmosphere, *Appl. Opt.*, *33*, 1760–1770, 1994.

Herman, B., T. R. Caudill, D. E. Flittner, K. J. Thome, and A. Ben-David, A comparison of the Gauss-Seidel spherical polarized radiative transfer code with other radiative transfer codes, *Appl. Opt.*, *33*, 4563–4572, 1995.

Karp, A. H., Computing the angular dependence of the radiation of a planetary atmosphere, *J. Quant. Spectrosc.*, *25*, 403–412, 1981.

Karp, A. H., and S. Petrack, On the spherical harmonics and discrete ordinates methods for azimuth-dependent intensity calculations, *J. Quant. Spectrosc.*, *30*, 351–356, 1983.

Mateer, C. L., and J. J. DeLuisi, A new Umkehr inversion algorithm, *J. Atmos. Ter. Phys.*, *54*, 537–556, 1992.

Mishchenko, M. I., A. A. Lacis, and L. D. Travis, Errors induced by the neglect of polarization in radiance calculations for Rayleigh-scattering atmospheres, *J. Quant. Spectrosc. Radiat. Transfer*, *51*, 491–510, 1994.

Nakajima, T., M. Tanaka, and T. Yamauchi, Retrieval of the optical properties of aerosols from aureole and extinction data, *Appl. Opt.*, *22*, 2951–2959, 1983.

Newchurch, M. J., and D. M. Cunnold, Aerosol effect on Umkehr ozone profiles using Stratospheric Aerosol and Gas Experiment II measurements, *J. Geophys. Res.*, *99*, 1383–1388, 1994.

Newchurch, M. J., D. M. Cunnold, and J. Cao, Intercomparison of SAGE with Umkehr[64] and Umkehr[92] ozone profiles and time series: 1979–1991, *J. Geophys. Res.*, *103*, 31,277–31,292, 1998.

Petropavlovskikh, I. V., J. J. DeLuisi, D. Theisen, L. Flynn, and B. Chu, Investigation of systematic and rms differences among ozone profiles observed by the Umkehr, SBUV, and SAGE, *J. Geophys. Res.*, in press, 1999.

Stamnes, K., On the computation of angular distributions of radiation in planetary atmospheres, *J. Quan. Spec.*, *28*, 47–51, 1982.

Tonna, G., T. Nakajima, and R. Rao, Aerosol features retrieved from solar aureole data: A simulation study concerning a turbid atmosphere, *Appl. Opt.*, *34*, 4486–4499, 1995.

J. DeLuisi, NOAA/ERL/ARL/SRRB, Boulder, CO 80303. (deluisi@srrb.noaa.gov)

B. Herman, University of Arizona, Tucson, AZ 85721. (herman@atmo.arizona.edu)

R. Loughman, Cooperative Center for Atmospheric Science and Technology, University of Arizona, Tucson, AZ 85721. (loughman@wrabbit.gsfc.nasa.gov)

I. V. Petropavlovskikh, NOAA, R/E/ARXL, 325 Broadway, Boulder, CO 80027. (irina@srrb.noaa.gov)